Pharmaceutical Informatics Institute, College of Pharmaceutical Sciences, Zhejiang University, Hangzhou, China

Astragalus membranaceus extract promotes neovascularisation by VEGF pathway in rat model of ischemic injury

LING ZHANG, YINGXIN YANG, YI WANG, XIUMEI GAO

Received August 9, 2010, accepted September 14, 2010

Yi Wang, Ph.D. Yuhangtang Road 388#, Zhejiang University, College of Pharmaceutical Sciences, Hangzhou, China mysky@zju.edu.cn.

Pharmazie 66: 144–150 (2011) *doi: 10.1691/ph.2011.0738*

Astragalus membranaceus extract (AME) is a widely used herbal product for the treatment of cardiovascular diseases in China. The present study aimed to evaluate the cardiac protective effects of AME, and to probe the underlying molecular mechanism related to angiogenesis. In this study, AME with 75 μg/mL significantly increased proliferation, migration and tube formation on human umbilical vein endothelial cells (HUVECs). Moreover, *in vivo* experiments on rats with ligation of left anterior descending artery were performed to study the cardiac protective and angiogenic effect of AME (50 and 100 mg/kg *i. g.* for 3, 7, 14 days). The results showed that AME inhibited cardiac fibrosis, reduced infarct size, and increased capillary and arteriole densities. Meanwhile, western blot was used to determine protein levels of VEGF, p-AKT, p-GSK3β and p-mTOR. AME significantly elevated protein expression of VEGF and increased phosphorylation of AKT, GSK3β and mTOR. In conclusion, AME exerted cardiac protective and angiogenic effects in the ischemic injured heart. The activation of AKT/GSK3β and AKT/mTOR pathways and elevated expression of VEGF may contribute to the promoted neovascularisation by AME.

1. Introduction

Astragalus membranaceus is a commonly used herb in the oriental medicinal system of China (Chen et al. 2005). In recent years, research focussed the cardiac protective effects of *Astragalus membranaceus* from both phytochemistry practitioners and pharmacologists. It has been reported that, *Astragalus membranaceus* can suppress cardiac functional dysfunction and morphological aberrations in experimental autoimmune myocarditis (Zhao et al. 2008), and eliminate doxorubicin induced cardiotoxicity by decreasing free radical release (Luo et al. 2009). Clinical studies showed that *Astragalus* significantly improved left ventricular function in 43 patients with acute myocardial infarction, and increased cardiac output of 20 individuals with angina (Miller 1998). Those pharmacological and clinical observations indicate that AME has the potential for treating cardiovascular diseases. However, the underlying mechanism for the cardiac protective effects of AME remains elusive.

Therapeutic angiogenesis has emerged as a new means for treating cardiovascular disease, which aims at stimulating collateral formation and improving myocardial perfusion (Becker et al. 2006). This novel strategy may be particularly beneficial for patients who are not candidates for conventional revascularization techniques such as angioplasty or bypass (Koneru et al. 2008). VEGF which stimulates migration, proliferation and tube formation is an giogeneic factor that plays a important role in angiogenesis (Singh et al. 2007). Phosphatidylinositol-3 kinase (PI3K)–Akt signaling axis in endothelial cells is activated by many angiogenic growth factors such as VEGF, angiopoietins-1, and it regulates downstream targets that are potentially involved in blood vessel growth and homeostasis (Shiojima and Walsh 2002). Therefore, PI3K–Akt signal pathway has received considerable attention in VEGF-stimulated angiogenesis research (Ferrara et al. 2003).

Our previous study has demonstrated that the Chinese medicinal formula Qi-Shen-Yi-Qi, in which *Astragalus membranaceus* is used as principle component, can induce angiogenic effects *in vivo* (Zhang et al. 2010). Meanwhile, due to the efficacy of *Astragalus membranaceus* for treating cardiovascular disease, we raised the hypothesis that AME may exert therapeutic effects on myocardial infarction through the angiogenesis pathway. In this study, *in vivo* and *in vitro* experiments were performed to provide a mechanistic insight into the cardiovascular therapeutic effects of AME.

2. Investigations and results

2.1. AME induces endothelial cells proliferation, migration and tube formation

The effects of AME on HUVEC proliferation in various concentrations (25, 50, 75 and 100 μg/mL) were measured in our study (Fig. 1). After exposure of HUVEC to AME for 48 h, significant increase of HUVEC proliferation was observed at the concentration of 75 μg/mL.

In the process of angiogenesis, quiescent endothelial cells are activated by some pro-angiogenic signal, they become highly proliferative and able to migrate, remodel the surrounding extracellular matrix (ECM) and differentiate to form new vessels (Cárdenas et al. 2006). Transwell culture chambers were used to assess whether AME promotes HUVEC migration. The result showed that VEGF (10 ng/mL) stimulated cells migrating to the lower surface of the membrane, whereas the cell with DMSO treatment remained at the upper wells (Fig. 2A and C). Similarly,

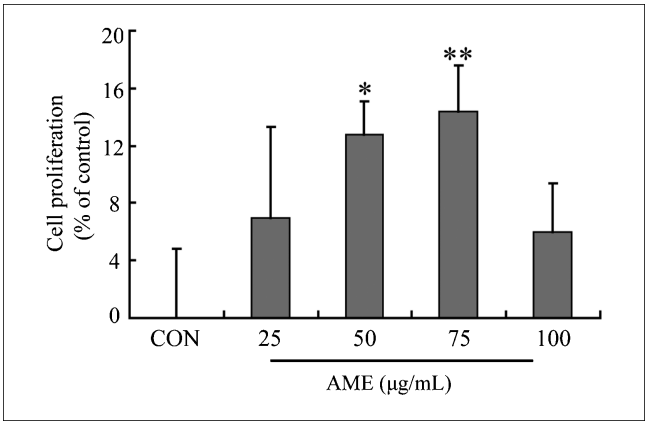

Fig. 1: Effects of AME on HUVEC proliferation. Cells were incubated in the presence or absence of various concentrations of AME for 48 h. Cell growth was evaluated by MTT assay and the percentage of stimulation was calculated by comparing to the control. Data are expressed as mean ± SEM. (n = 4, for each experimental group), ** $P < 0.01$ vs. CON; * $P < 0.05$ vs. CON

AME enhanced cell migration at the concentration of 75 μg/mL (Fig. 2A and C).

The effect of AME on tube formation was evaluated by Matrigel. As the photos show, HUVECs stimulated with AME (75 μg/mL) or VEGF (10 ng/mL) formed elongated capillary-like tubes and complete networks within 7 h, while the control culture developed small amounts of capillary-like structures and incomplete networks (Fig. 2B and D).

2.2. *AME inhibits cardiac fibrosis and infarct size*

To determine the effect of AME on cardiac fibrosis, fibrotic areas were stained blue with Masson's trichrome in the myocardial sections. Fig. 3A shows that both fibrosis and ventricular dilatation increased in occlusion heart after 3, 7 and 14 days. Compared to a large MI heart with fibrosis and ventricular dilatation in the MI group, AME-treated heart, especially the high dose

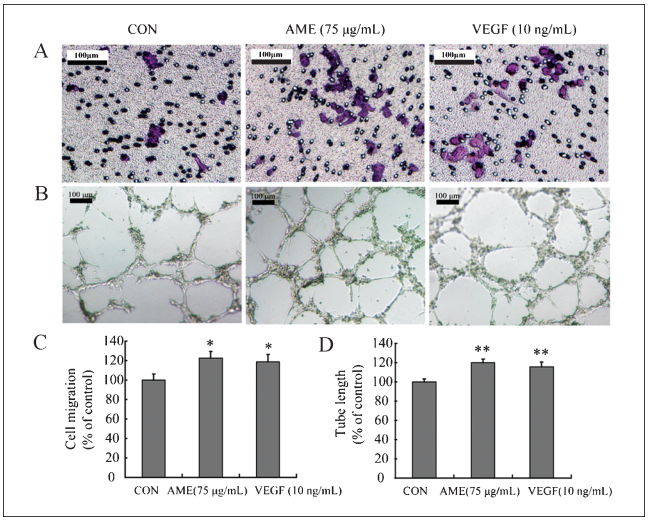

Fig. 2: Effect of AME on cell migration and tube formation. (A) Migration assay was carried out with transwell culture chambers. Cells in transwell were treated for 24 h, the cells migrating to the lower surface of the membrane were stained with 0.1% crystal violet and examined (original magnification × 200). Bar indicates 100 μm. (B) tube formation was evaluated by Matrigel. Cells were treated for 7 h and capillary like structures were examined at magnification × 100. (C) Six different areas of migrated cells were counted for each data point. Data are expressed relative to the mean control value. (D) The total length of the vessels in five fields of each well was used for assessment and the values were expressed relative to the mean control value. Data are expressed as mean ± SEM. (n = 3, for each experimental group), ** $P < 0.05$ vs. CON; * $P < 0.05$ vs. CON

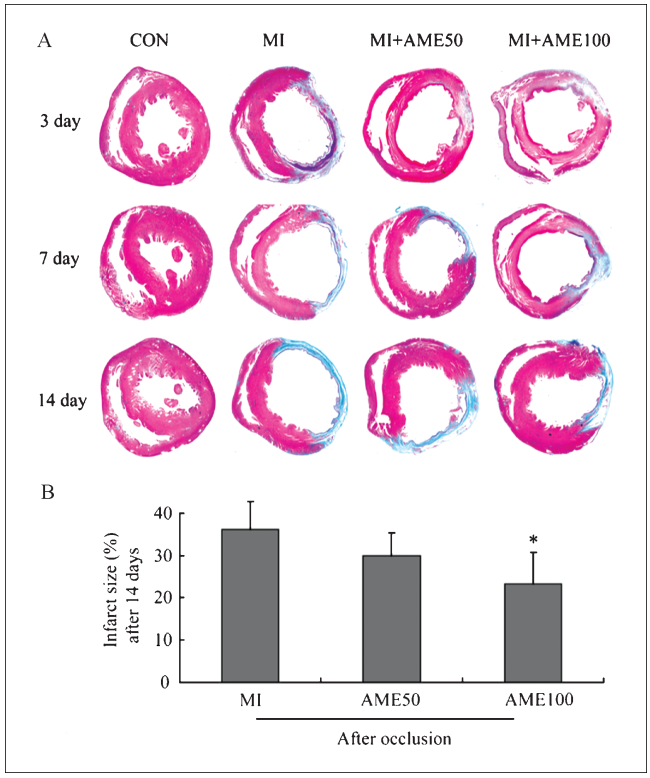

Fig. 3: Effect of AME on cardiac fibrosis and infarct size. (A) Masson's trichrome staining for identifies cardiac fibrosis. Original magnification is ×10. (B) TTC staining for infarct size in MI group, 50 μg/mL and 100 μg/mL AME-treated groups on day 14. Values are expressed as mean ± SEM. (n = 8, for each experimental group), *$P < 0.05$ vs. MI

treatment heart, showed a smaller MI with less fibrosis after 3, 7, and 14 days. Additionally, the infarct area stained with TTC on day 14 was similar to that stained with Masson's trichrome (Fig. 3B). Compared with the MI group, infarct size was significantly reduced after 14 days in the hearts of the 100 mg/kg AME-treated group (36.1 ± 6.7% vs. 23.3 ± 7.4%, $P < 0.05$). The data suggested that AME reversed LV remodeling in MI rats.

2.3. *AME increases capillary and arteriolar density*

Since AME promoted angiogenesis notably *in vitro*, we tried to investigate whether angiogenesis contribute to cardio protection *in vivo* by vWF and α-SMA staining. Capillary density was determined by immunohistochemical stained with anti-vWF in the peri-infarct area (Fig. 4A). The data showed that capillary density in 50 mg/kg and 100 mg/kg AME treated groups was increased after 3, 7, and 14 days. Of note, AME (100 mg/kg) treatment group's capillary density significantly increased by about 1.9-fold compared with MI group ($P < 0.05$) on day 7. On day 14, the capillary density of 50 mg/kg and 100 mg/kg AME treatment group were both notably raised compared with the MI group (1.6-fold in 50 mg/kg AME group, $P < 0.05$; 2-fold in 100 mg/kg AME group, $P < 0.01$) (Fig. 4C). Furthermore, small arterioles in the tissue sections were stained with an antibody against a-smooth muscle actin (Fig. 4B). Quantification indicated that arteriolar density was significantly higher in 50 mg/kg and 100 mg/kg AME treatment group on day 7 compared with the MI group by approximately 1.4-fold ($P < 0.05$) and 1.7-fold ($P < 0.05$). On day 14, arteriolar density was also notably increased in 50 mg/kg and 100 mg/kg AME treatment groups compared with MI (1.6-fold in 50 mg/kg AME group, $P < 0.01$; 2-fold in 100 mg/kg AME group, $P < 0.01$) (Fig. 4D). These findings suggest that AME promotes angiogenesis in the peri-infarct area *in vivo*.

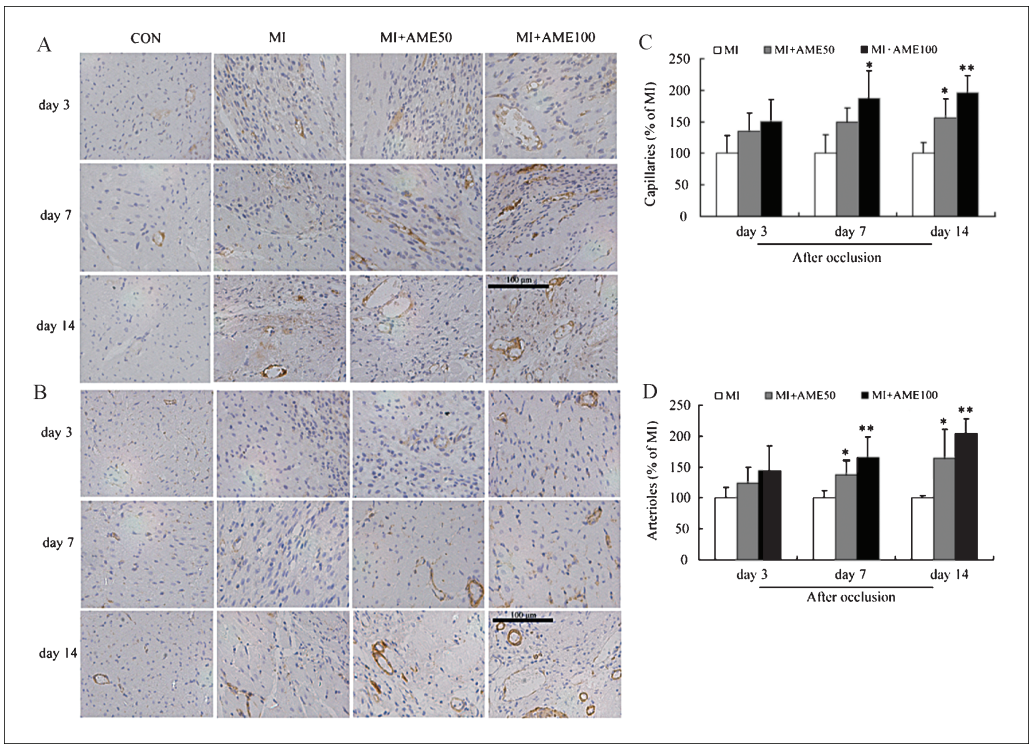

Fig. 4: Effects of AME on capillary densities and arteriole densities. (A) Immunostaining for vWF identifies capillaries. Bar indicates 100 μm. (B) Immunostaining for α-SMA identifies arterioles. Bar indicates 100 μm. (C) Quantitative analysis of capillary density in the peri-infarct myocardium. Original magnification is ×400. (D) Quantitative analysis of arteriolar density in the peri-infarct myocardium. Original magnification is ×400. The total number of the vessels in five different areas of one section was used for the assessment of vascular density and the data was expressed relative to the model value. Values are expressed as mean ± SEM (n = 4, for each experimental group), ** $P < 0.01$ vs. MI; * $P < 0.05$ vs. MI

2.4. Effect of AME on expression of angiogenic proteins

A series of factors involved in the pathway of angiogenesis including VEGF, p-AKT/AKT, p-GSK 3β/GSK 3β and p-mTOR/mTOR were determined by Western blot. VEGF, an angiogenic growth factor, seems to be important in angiogenesis. The result showed that VEGF expression in MI group dropped below control on day 7 and day 14 after a spontaneous increase on day 3. While VEGF expression in the 100 mg/kg AME treatment group was significantly increased on day 7 and day 14 by about 2 fold ($P < 0.05$) and 1.8 fold ($P < 0.05$) compared with the MI group (Fig. 5A and B).

AKT, which acts as a downstream target in VEGF pathway, is involved in many regulatory pathways in myocardial pathological developments. We examined AKT protein expression and its phosphorylation at Ser473 in MI hearts with or without AME treatment (Fig. 5C and D). The expression of p-AKT was up-regulated in the 100 mg/kg AME treatment group in a time-dependent manner. On day 14, the p-AKT protein level was notably elevated in 100 mg/kg AME treatment group by about 1.7-fold ($P < 0.05$) compared with the MI group (Fig. 5C and D). Recently, Glycogen synthase kinase-3β (GSK3β) is deemed to play a key role in endothelial cells by regulating vessel growth through its control of vascular cell migration and survival (Kim et al. 2002). AKT can mediate GSK3β phosphorylation at Ser9 to inactivate GSK3β and promotes angiogenesis. In our study, we found that the phosphorylation level of GSK3β increased in a time-dependent manner in the MI group compared with control group. On day 7, 100 mg/kg AME notably up-regulated the protein level of p-GSK3β by 1.9-fold ($P < 0.05$) compared with MI group. On day 14, p-GSK3β expression was also significantly increased in 50 mg/kg and 100 mg/kg AME treatment groups by 1.6-fold ($P < 0.05$) and 1.7-fold ($P < 0.01$) compared with the MI group (Fig. 6A and B).

Activation of mTOR is an important regulatory mechanism for cellular protein synthesis and cardiac hypertrophy (Braz et al. 2009). In our study, the phosphorylation level of mTOR at ser2448 increased in the MI group compared with the control group on day 3, 7 and 14. On day 14, the protein level of p-mTOR notably raised in 100 mg/kg AME treatment group by about 2-fold compared with MI group ($P < 0.05$) (Fig. 6C and D).

3. Discussion

Briefly, we investigated the cardioprotective effect of AME and its possible mechanism. AME significantly stimulated proliferation, migration and tube formation in HUVECs, and remarkably increased myocardial capillary and arteriolar density in the peri-infarct area, both suggesting that AME promoted the formation of functional microvessels leading to increased blood flow in the infarcted heart. Furthermore, angiogenesis, which may rely on activation of VEGF and the PI3K/AKT pathway, is implicated in the cardioprotective effect of AME.

Indes hypoxic conditions such as myocardial ischemia, the expression and secretion of VEGF is up-regulated spontaneously in the myocardial cell. It was also observed in our study that protein expression of VEGF increased in MI at day 3. But the short term elevated expression of VEGF was found to generate immature vessels that regressed later, whereas longer-term VEGF expression would lead to stable and persistent vessels (von Degeasfeld et al. 2003). This research found that the VEGF protein level was still increased in AME treatment group at day 7 and 14, but decreased in the MI group. Thus, AME can promote the myocardial cell to form mature vessels by increasing the expression VEGF protein in a long term.

AKT, a cardinal intracellular kinase, regulates various functions in the heart, whose phosphorylation at ser473 is important in the cardiomyocytes mediated by mammalian target of rapamycin complex 2 and P21-activated kinase-1 (Mao et al. 2008). In our study, phosphorylation expression of AKT at ser473 was observed to increase notably in AME treatment group compared

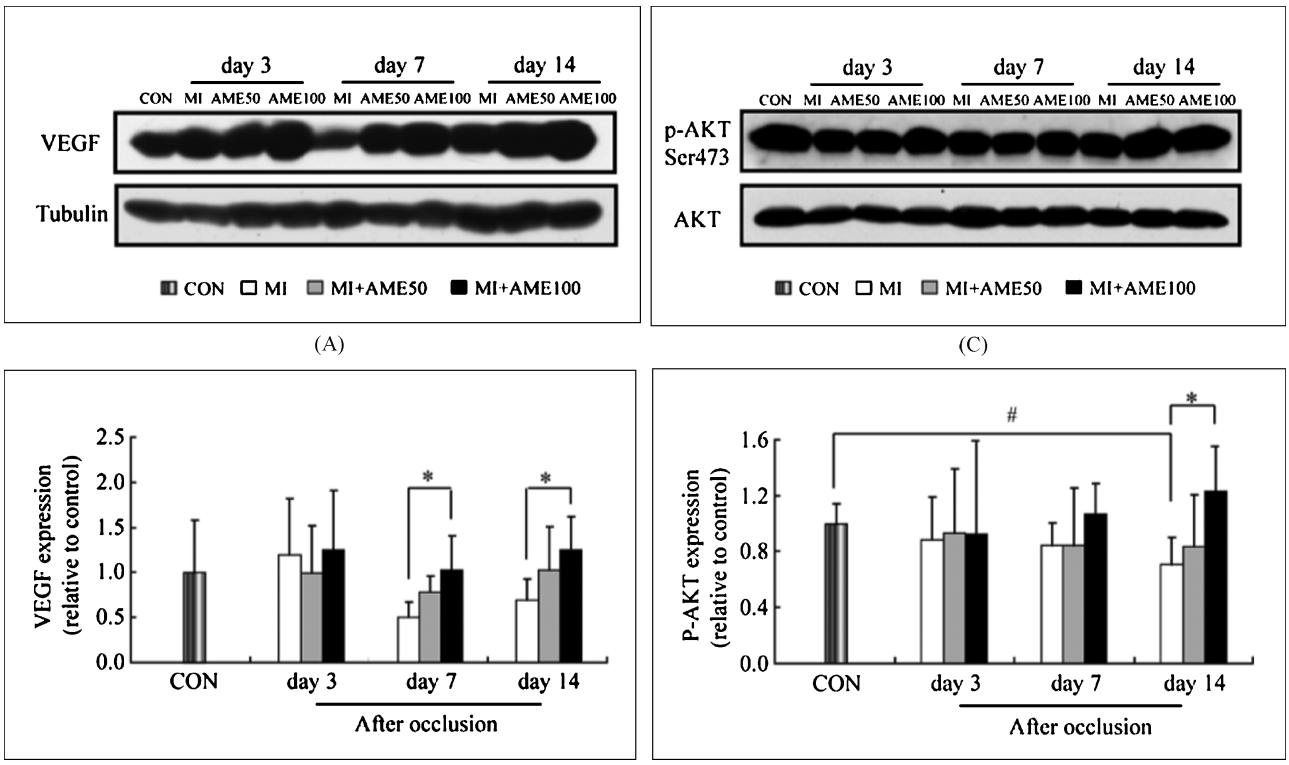

Fig. 5: Effect of AME on VEGF expression and p-AKT/AKT expression. (A) Expression of VEGF and tubulin in the heart tissues dissected from rats of CON, MI, MI + AME50 and MI + AME100 group after 3, 7 and 14 days. (B) VEGF expession was expressed by ratio of VEGF/Tubulin (n = 4; for each experimental group). (C) The expression of total AKT and p-AKT in the hearts of CON, MI, MI + AME50 and MI + AME100 groups after 3, 7 and 14 days. (D) AKT activity was expressed by ratio of p-AKT/AKT (n = 4; for each experimental group). * $P < 0.05$ vs. MI; # $P < 0.05$ vs. CON

with MI group at 14 days. The data suggested that AKT was implicated in the pro-angiogenic effect of AME.

AKT-GSK3β signaling regulated vessel growth independent from the AKT-eNOS regulatory axis which promoted endothelium-dependent relaxation in a redox-sensitive manner (Kim et al. 2002; Anselm et al. 2009). To the best of our knowledge, little is known about the role of GSK3β signaling in the cardiovascular system. In cell culture studies, Skurk et al. (2005) showed that the growth factor–PI3K–AKT axis functions downstream of GSK3β-β-catenin signaling in HUVECs to promote

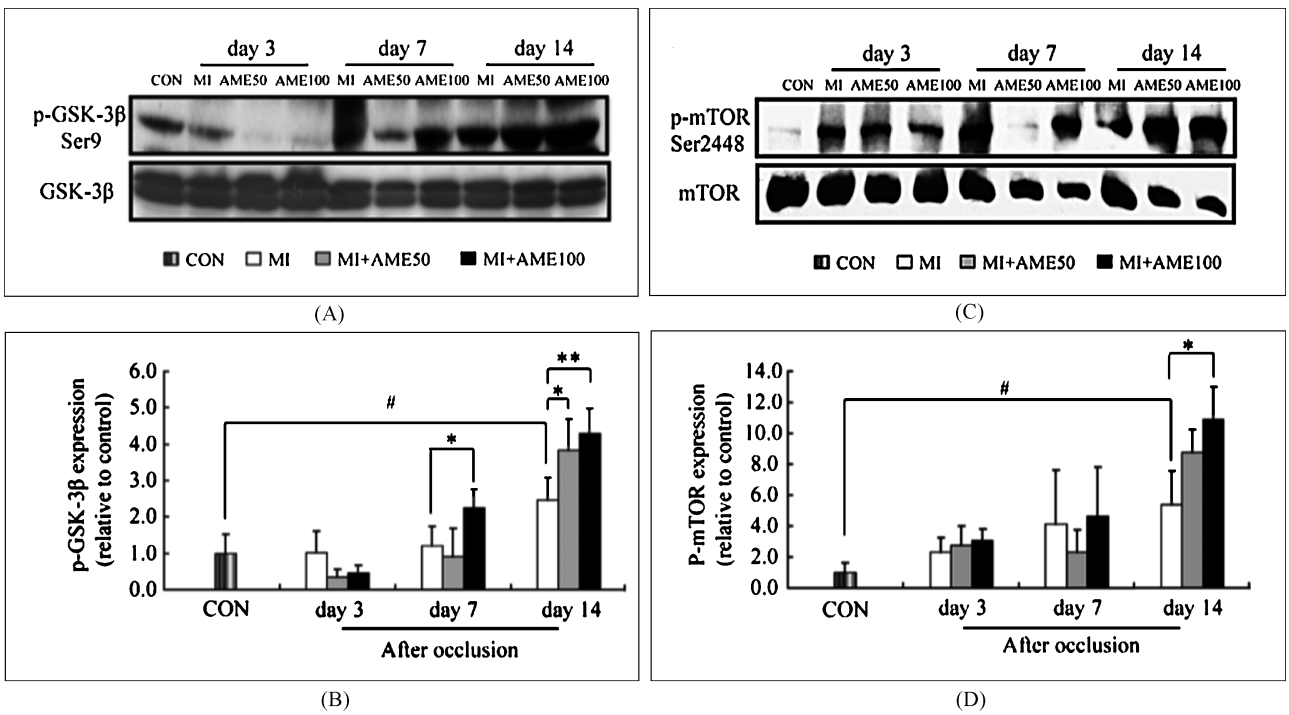

Fig. 6: Effect of AME on p-GSK 3β/GSK 3β expression and p-mTOR/mTOR expression. (A) GSK 3β and p-GSK 3β in protein extracts from CON, MI, MI + AME50 and MI + AME100 hearts after 3, 7 and 14 days. (B) GSK 3β expression was expressed by ratio of p-GSK 3β/GSK 3β (n = 4; for each experimental group). (C) mTOR and p-mTOR in heart extracts from CON, MI, MI + AME50 and MI + AME100 group after 3, 7 and 14 days. (D) mTOR expression was expressed by ratio of p-mTOR/mTOR (n = 4; for each experimental group), ** P < 0.01 vs. MI; * $P < 0.05$ vs. MI; # $P < 0.05$ vs. CON

angiogenesis. Yao et al. (2008) suggested that tissue kallikrein protected against acute phase MI by promoting neovascularization through the kinin B2 receptor-AKT-GSK3β and VEGF signaling pathways. In this study, AME increased the phosphorylation level of GSK3β at Ser9, which indicated the inactivation of GSK3β and promoting angiogenesis. mTOR was also the downstream of AKT, which belongs to a evolutionarily conserved member of the phosphatidylinositol kinase-related kinase family whose phosphorylation can activate the downstreams, thus leading to translation of regulation protein, cell growth, and proliferation (Braz et al. 2009; Fingar et al. 2002). In hypoxia condition, mTOR signaling to cell proliferation and angiogenesis was augmented (Humar et al. 2002). The report showed that mTOR phosphorylation on Ser2448 but not Ser2481 was modulated in the pathophysiological O_2 concentration range (Li et al. 2007). AME was found to raise the protein level of p-mTOR at ser2448 on day 14. This result further testified that the angiogenesis induced by AME was through AKT signaling. Taken together, the results of this study indicate that AME promotes angiogenesis to prevent LV remodeling in MI by up-regulating VEGF, p-AKT, p-GSK3β and p-mTOR protein levels.

In conclusion, our research provided evidence that AME promotes the formation of functional microvessels, which led to increased blood flow in the infarcted heart. Enhanced expression of VEGF and activation of AKT-GSK3β and AKT-mTOR pathway may be involved in pro-angiogenic effect of AME. These findings will contribute to develop new therapeutical angiogenic agents from natural products for the treatment of coronary heart diseases and provide a proof for dissection of the Chinese medicinal formula QI-SHEN-YI-QI.

4. Experimental

4.1. Preparation and analysis of AME

AME powder was purchased from Ruikang Bio-engineering Co (Xian, China). The extract used in our study was manufactured according to the standardized preparation method as follows. Briefly, dried, powdered roots of *Astragalus membranaceus* were soaked in water for 2 h at 45 °C, then refluxed with water three times. The extracts were combined and evaporated to yield an extract with a density ranging from 1.35 to 1.40. Distilled water was added to precipitate for 24-48 h. The supernatant was removed and evaporated to obtain an extract with a density ranging from 1.1 to 1.2. Afterwards, the extracts were spray dried, pulverized, and sifted (100 mesh). The AME aqueous solution (40 mg/mL) was further purified by solid-phase extraction (SPE). A SPE cartridge (YMC C_{18}, 200 mg) was conditioned with 3 mL methanol and equilibrated with 2 mL water. Then 0.2 mL of AME aqueous solution was loaded onto the column. After being washed with 1 mL water and 1 mL 50% methanol, the wash solution by 50% methanol was collected for HPLC/MS analysis.

HPLC analysis was performed on an Agilent 1100 HPLC instrument (Agilent, Waldbronn, Germany) coupled with a binary pump, an auto-sampler, and a column compartment. The samples were separated on an Ultimate^{TM} XB-C_{18} column, 5 μm, 250 mm × 4.6 mm i.d. (Welch Materials, Inc., Ellicott, MD, USA). The mobile phase was a stepwise gradient of water (containing 0.05% formic acid, v/v) and acetonitrile. A Finnigan LCQ Deca XP^{plus} ion trap mass spectrometer (Thermo Finnigan, San Jose, CA, USA) was connected to the Agilent 1100 HPLC instrument via an ESI interface. Representative TIC chromatogram of AME and structures of major constituents were shown in Fig. 7.

4.2. Cell culture

Primary human umbilical vein endothelial cells (HUVEC) were isolated, grown, and identified as described earlier (Hermenegildo et al. 2005). HUVECs at passages 4–8 were cultured on gelatin-coated flasks in Medium 199 (M199, Gibco, Grand Island, NY, USA) supplemented with 12.5% fetal bovine serum (FBS, Gibco, Grand Island, NY, USA), 50 U/mL heparin (Shanghai No. 1 Biochemical Pharmaceutical Co, Shanghai, China), 30 μg/mL ECGS (BD, New Jersey, NY, USA), 10 ng/mL EGF (BD, New Jersey, NY, USA) and 100 U/mL penicillin (Zhongguo pharmaceutical (shijiazhuang) co, Hebei, China) and streptomycin (Northern China pharmaceutical co, shijiazhuang, Hebei, China). The investigation conforms to the principles outlined in the Declaration of Helsinki. The Ethics Committee of the Medical College of Zhejiang University approved all procedures.

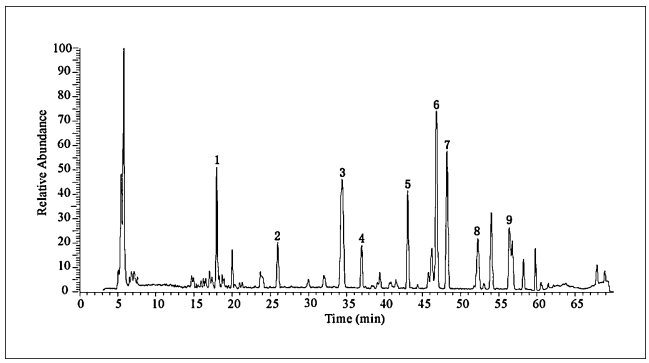

Fig. 7: Total ion current chromatogram of AME by HPLC/MS analysis. Peaks 1 calycosin-7-O-β-D-gluoside; 2, ononin; 3, calycosin; 4, astragaloside VII; 5, astragaloside V; 6, astragaloside IV; 7, astragaloside III, 8, formononetin; 9, soyasaponin I

4.3. HUVEC proliferation assay

HUVECs were cultured on collagen-coated 96-well plates at a density of 2×10^4 cells/well for 48 h. Then the cells were treated with testing samples by replacing the media with 0.1 mL M199 containing 2% FBS. The growth medium was supplemented with AME at a series of concentrations (25, 50, 75 and 100 μg/mL). DMSO was added as a control. After the cells had been incubated for 48 h, cell numbers were estimated by the MTT [3-(4,5-dimeth-ylthiazol-2-yl)-2,5-diphenyl-tetrazolium bromide] assay (Pozzolini et al. 2003). Briefly, The MTT labeling reagent (5 mg/mL MTT in PBS, Sigma, Ronkonkoma, NY, USA) was added to the culture to obtain the final concentration of 0.5 mg/mL, and the culture was incubated for 4 h. The media were removed and formazan crystals were solubilized with 175 μL DMSO. Each well was measured at 550 nm for by Universal Microplate Spectrophotometer (Bio-Tek, Winooski, VT, USA). Cell proliferation rate (percentage of control) = ($A_{550\ nm}$ of the AME treatment - $A_{550\ nm}$ of the control)/$A_{550\ nm}$ of the control × 100%.

4.4. HUVEC transwell migration assay

The effect of AME on HUVECs migration was determined by a transwell migration assay as previously described (Redmond et al. 1999). Briefly, HUVECs were seeded (1×10^5 cells/well) into the upper reservoir of a transwell chemotaxis chamber (24-well culture plates, Corning, NY, USA) containing 2% FBS growth media, whilst the lower reservoir was supplemented with DMSO (serve as control), 75 μg/mL AME or 10 ng/mL VEGF. HUVECs were subsequently allowed to migrate across a fibronectin-coated polycarbonate filter (8 μm pore) for 24 h in a humidified atmosphere of 5% CO_2/95% air at 37 °C. Non-migrated cells were removed from the top side of the filter by washing thrice in PBS and scraping gently. Migrated cells on the bottom side of the filter were subsequently fixed with 10% formaldehyde for 30 min and then stained with 0.1% crystal violet for 20 min. Five fields were counted for each well.

4.5. HUVEC tube formation

A Matrigel tube formation assay was also performed to assess *in vitro* angiogenesis. Growth factor–reduced Matrigel (BD, New Jersey, NY, USA) was placed in 96-well culture plates (50 μL/well) and allowed to set at 37 °C for 1 h. Then 1×10^4 HUVECs were added to each well and incubated in 2% FBS M199 basic medium with 75 μg/mL AME, 10 ng/mL VEGF or DMSO for 7 h in a humidified atmosphere of 5% CO_2/95% air at 37 °C. Five fields were counted for each well. The length of the tube was measured by Image-Proplus 6.0 (Media Cybernetics, Bethesda, MD, USA).

4.6. Induction of myocardial infarction in rats and drug treatment

Male Sprague-Dawley rats (220∼250 g) were purchased from Shanghai slaccas Experimental Animal Co (SCXK-2007-0005). All rats were fed with a standard laboratory diet and given free access to tap water, kept in a controlled room temperature (22 ± 1 °C), humidity (65-70%), and 12 h dark/light cycles for 1 week before experiments began. The investigation conforms to the Guide for the Care and Use of Laboratory Animals published by the US National Institutes of Health (NIH Publication No. 85-23, revised 1996). The Animal Ethic Review Committees of Zhejiang University approved all procedures.

Myocardial infarction models were produced by occlusion of the left anterior descending coronary artery according to the method of Yamaguchi (Pfeffer et al. 1979; Yamaguchi et al. 1997). Briefly, the rats were anesthetized with sodium pentobarbital by intraperitoneal injection (50 mg/kg i.p.) and ventilated by a respirator (ALC-V8, Shanghai Alcott Biotech, Shanghai, China)

with room air (tidal volume, 3 mL/100 g; respiratory rate, 60 cycles/min). A thoracotomy was performed in the fourth intercostal space and a 5/0 Proline suture was tied around the left anterior descending coronary artery a few millimeters from its origin. In sham-operated rats, the ligation suture was not placed in the heart. Following ligation or sham surgery, rats were randomly assigned to four groups and treated orally as follows: control group (CON), water treatment; myocardial infarction group (MI), water treatment; MI + AME50 group, 50 mg/kg AME consecutively for 3, 7 and 14 days; MI + AME100 group, 100 mg/kg AME consecutively for 3, 7 and 14 days.

4.7. Histological analysis

The heart was rapidly excised and fixed in neutral buffered formalin after 3, 7 and 14 days, then it was embedded in paraffin, three slices from the left ventricle were obtained for morphological analyses, Masson's trichrome staining was performed to show the collagen formation after MI. Immunohistochemistry was performed to determine capillaries and small arteries in the peri-infarct area using primary antibody: rabbit anti human von Willebrand factor (vWF, Chemicon, Temecula, CA, USA, 1 mg/ml to 10 μg/mL) and α-smooth muscle actin (α-SMA, Epitomics; Burlingame, CA, USA, 1:200), then incubated with corresponding biotinylated secondary antibody (Shanghai gene company, Shanghai, China) and DAB kit (Zhongshan goldenbridge, Beijing, China). The number of positive staining of each section was counted in 5 different fields from the peri-infarct area.

4.8. Infarct size measurement

Infarct size of heart was measured on day 14 after infarction. Briefly, the heart was rapidly excised and serially sectioned into five slices (1 mm thick). The slices were then incubated in 1% triphenyltetrazolium chloride (TTC, Sigma, St. Louis, MO, USA) for 5 min at 37 °C to distinguish non-infarct tissue and infarct tissue (the area lacking TTC staining, IA). The corresponding areas were weighed. The infarction area as a percent ratio of the left ventricular mass was calculated as: IA/LV = weight of infarct area/weight of left ventricle × 100%.

4.9. Western blot analysis

After 3, 7 and 14 days, heart samples in the border zone from the left ventricle were homogenized in lysis buffer as described by Wang et al. (2003). The protein content of the supernatants was determined by the Bradford protein assay. Western blots were performed for total and phosphorylated AKT, VEGF, total and phosphorylated GSK-3β, total and phosphorylated mTOR (VEGF-specific antibody, diluted 1:500, Santa Cruz, Santa Cruz, CA, USA. AKT-specific antibody, diluted 1:1000, p-AKT-specific antibody, diluted 1:1000, Cell Signalling Technology, Frankfurt, Germany. GSK3β-specific antibody, diluted 1:1000, p-GSK3β-specific antibody, diluted 1:500, mTOR-specific antibody, diluted 1:500, p-mTOR-specific antibody, diluted 1:250, Millipore, Billerica, MA, USA). VEGF/Tubulin, p-AKT/AKT, p-GSK3β/GSK3β, and p-mTOR/mTOR ratios were expressed relative to the mean control value.

4.10. Data analysis

Data were expressed as mean ± SEM. n, the number of individual experiments. Statistical analysis was performed using one-way ANOVA. *P*-values of < 0.05 were considered significant. All statistical analyses were performed by MINITAB 14 (Mintab Inc, State College, PA, USA).

Acknowledgements: This work was supported by the key grant from National Natural Science Foundation of China (Grant number 30830121, 30801461), and grant from National Key Scientific and Technological Project of China (Grant number 2009ZX09311-002). The authors wish to thank Associate Prof. Youfa Zhu (Department of Pathology, Zhejiang University School of Medicine) and PhD. Peiying Shi (Department of Chinese Medicine Science & Engineering, College of Pharmaceutical Sciences, Zhejiang University) for technical helps.

References

Anselm E, Socorro VF, Dal-Ros S, Schott C, Bronner C, Schini-Kerth VB (2009) Crataegus special extract WS 1442 causes endothelium-dependent relaxation via a redox-sensitive Src- and Akt-dependent activation of endothelial NO synthase but not via activation of estrogen receptors. J Cardiovasc Pharmacol 53: 253–260.

Becker C, Lacchini S, Muotri AR, da Silva GJ, Castelli JB, Vassallo PF, Menck CF, Krieger JE (2006) Skeletal muscle cells expressing VEGF induce capillary formation and reduce cardiac injury in rats. Int J Cardiol 113: 348–354.

Braz JC, Gill RM, Corbly AK, Jones BD, Jin N, Vlahos CJ, Wu Q, Shen W (2009) Selective activation of PI3Kalpha/Akt/GSK-3beta signalling and cardiac compensatory hypertrophy during recovery from heart failure. Eur J Heart Fail 11: 739–748.

Cárdenas C, Quesada AR, Medina MA (2006) Evaluation of the anti-angiogenic effect of aloe-emodin. Mol Life Sci 63: 3083–3089.

Chen G, Wang XL, Wong WS, Liu XD, Xia B, Li N (2005) Application of 3' untranslated region (UTR) sequence-based amplified polymorphism analysis in the rapid authentication of Radix astragali. J Agric Food Chem 53: 8551–8556.

Ferrara N, Gerber HP, LeCouter J (2003) The biology of VEGF and its receptors. Nat Med 9: 669–676.

Fingar DC, Salama S, Tsou C, Harlow E, Blenis J (2002) Mammalian cell size is controlled by mTOR and its downstream targets S6K1 and 4EBP1/eIF4E. Genes Dev 16: 1472–1487.

Hermenegildo C, Oviedo PJ, García-Pérez MA, Tarín JJ, Cano A (2005) Effects of phytoestrogens genistein and daidzein on prostacyclin production by human endothelial cells. J Pharmacol Exp Ther 315: 722–728.

Humar R, Kiefer FN, Berns H, Resink TJ, Battegay EJ (2002) Hypoxia enhances vascular cell proliferation and angiogenesis *in vitro* via rapamycin (mTOR)-dependent signaling. FASEB J 16: 771–780.

Kim HS, Skurk C, Thomas SR, Bialik A, Suhara T, Kureishi Y, Birnbaum M, Keaney JF Jr, Walsh K (2002) Regulation of angiogenesis by glycogen synthase kinase-3beta. J Biol Chem 277: 41888–41896.

Koneru S, Varma Penumathsa S, Thirunavukkarasu M, Vidavalur R, Zhan L, Singal PK, Engelman RM, Das DK, Maulik N (2008) Sildenafil-mediated neovascularization and protection against myocardial ischaemia reperfusion injury in rats: role of VEGF/angiopoietin-1. J Cell Mol Med 12: 2651–2664.

Li W, Petrimpol M, Molle KD, Hall MN, Battegay EJ, Humar R (2007) Hypoxia-induced endothelial proliferation requires both mTORC1 and mTORC2. Circ Res 100: 79–87.

Luo Z, Zhong L, Han X, Wang H, Zhong J, Xuan Z (2009) Astragalus membranaceus prevents daunorubicin-induced apoptosis of cultured neonatal cardiomyocytes: role of free radical effect of Astragalus membranaceus on daunorubicin cardiotoxicity. Phytother Res 23: 761–767.

Mao K, Kobayashi S, Jaffer ZM, Huang Y, Volden P, Chernoff J, Liang Q (2008) Regulation of Akt/PKB activity by P21-activated kinase in cardiomyocytes. J Mol Cell Cardiol 44: 429–434.

Miller AL (1998) Botanical Influences on Cardiovascular Disease. Altern Med Rev 3: 422–431.

Pfeffer MA, Pfeffer JM, Fishbein MC, Fletcher PJ, Spadaro J, Kloner RA, Braunwald E (1979) Myocardial infarct size and ventricular function in rats. Circ Res 44: 503–512.

Pozzolini M, Scarfi S, Benatti U, Giovine M (2003) Interference in MTT cell viability assay in activated macrophage cell line. Anal Biochem 313: 338–341.

Redmond EM, Cahill PA, Hirsch M, Wang YN, Sitzmann JV, Okada SS (1999) Effect of pulse pressure on vascular smooth muscle cell migration: the role of urokinase and matrix metalloproteinase. Thromb Haemost 81: 293–300.

Shiojima I, Walsh K (2002) Role of Akt signaling in vascular homeostasis and angiogenesis. Circ Res 90: 1243–1250.

Singh AK, Sharma A, Warren J, Madhavan S, Steele K, RajeshKumar NV, Thangapazham RL, Sharma SC, Kulshreshtha DK, Gaddipati J, Maheshwari RK (2007) Picroliv accelerates epithelialization and angiogenesis in rat wounds. Planta Med 73: 251–256.

Skurk C, Maatz H, Rocnik E, Bialik A, Force T, Walsh K (2005) Glycogen-Synthase Kinase3beta/beta-catenin axis promotes angiogenesis through activation of vascular endothelial growth factor signaling in endothelial cells. Circ Res 96: 308–318.

von Degenfeld G, Banfi A, Springer ML, Blau HM (2003) Myoblast-mediated gene transfer for therapeutic angiogenesis and arteriogenesis. Br J Pharmacol 140: 620–626.

Wang XG, Zheng W, Christensen LP, Tomanek RJ (2003) DITPA stimulates bFGF, VEGF, angiopoietin, and Tie-2 and facilitates coronary arteriolar growth. Am J Physiol Heart Circ Physiol 284: 613–618.

Yamaguchi F, Sanbe A, Takeo S (1997) Cardiac sarcoplasmic reticular function in rats with chronic heart failure following myocardial infarction. J Mol Cell Cardiol 29: 53–63.

Yao YY, Yin H, Shen B, Smith RS Jr, Liu Y, Gao L, Chao L, Chao J (2008) Tissue kallikrein promotes neovascularization and improves cardiac func-

tion by the Akt-glycogen synthase kinase-3beta pathway. Cardiovasc Res 80: 354–364.

Zhang L, Wang Y, Yu L, Liu L, Qu H, Wang Y, Gao X, Zhang B, Cheng Y (2010) QI-SHEN-YI-QI accelerates angiogenesis after myocardial infarction in rats. Int J Cardiol 143: 105–109.

Zhao P, Su G, Xiao X, Hao E, Zhu X, Ren J (2008) Chinese medicinal herb Radix Astragali suppresses cardiac contractile dysfunction and inflammation in a rat model of autoimmune myocarditis. Toxicol Lett 182: 29–35.